

Similarity solutions for radiation in time-dependent relativistic flows

L. B. Lucy

Astrophysics Group, Blackett Laboratory, Imperial College London, Prince Consort Road, London SW7 2AZ, UK
e-mail: l.lucy@imperial.ac.uk

Received 24 August 2004 / Accepted 31 August 2004

Abstract. Exact analytic solutions are derived for radiation in time-dependent relativistic flows. The flows are spherically-symmetric homologous explosions or implosions of matter with a grey extinction coefficient. The solutions are suitable for testing numerical transfer codes, and this is illustrated for a fully relativistic Monte Carlo code.

Key words. radiative transfer – methods: analytical – methods: numerical

1. Introduction

In a recent paper (Lucy 2005), a Monte Carlo (MC) treatment accurate to $O(v/c)$ of the time-dependent transport of radiation in 3-D SNe is described and tested. A major concern in that paper is establishing the accuracy of the MC code. To this end, the 3-D code was applied to a 1-D problem that could be solved independently with conventional numerical methods. Specifically, the test problem was to compute the bolometric light curve of a spherical SN in which the transfer of UVOIR radiation is treated with a grey extinction coefficient. An independent approach to this problem is provided by Castor's (1972) co-moving frame (cmf) moment equations for spherically-symmetric flows. The resulting pair of partial differential equations (PDEs) were solved with the Henyey method.

The final outcome of this test was entirely satisfactory: the mean difference between the two light curves is $\lesssim 0.01$ mag. for elapsed times t from 10 to 50 days. Nevertheless, the differences were initially significant, and it was not clear which code was in error. This question was eventually answered by testing each code separately against an exact similarity solution of Castor's equations. The cause of the differences could then be traced to the poor spatial resolution of the MC code.

In the interest of concise presentation, the essential part played by this similarity solution was not described in the earlier paper (Lucy 2005). But subsequently, this solution was found to generalize to all orders of v/c . Accordingly, since time-dependent relativistic flows and the associated transfer problems are of interest for such phenomena as gamma-ray bursts and micro-quasars, this paper derives this solution (and variants thereof) and illustrates its use in testing a relativistic transfer code.

2. Basic equations

Similarity solutions will be sought for the frequency-integrated radiation field in a homologously expanding or contracting flow. The configuration is spherically-symmetric, and the matter has grey extinction (χ) and integrated emissivity (η) coefficients that are isotropic in the cmf.

2.1. The transfer equation

Mihalas (1980) has derived the general time-dependent cmf transfer equation for spherically-symmetric flows with relativistic velocities. From this, he derives the zeroth and first frequency-integrated moment equations, whose earlier derivation by Prokof'ev (1962) is acknowledged. When terms of $O(v^2/c^2)$ and higher are neglected, Castor's (1972) moment equations are recovered.

Following Mihalas (1980), the interaction coefficients (χ, η) and the radiation field (I, J, H, K) are expressed in the cmf but spacetime coordinates (r, t) and flow velocities (v) are measured in the rest frame (rf). Since radiation quantities always refer to the cmf, primes or suffixes to indicate this frame are omitted (cf. Mihalas 1980, Sect. III).

In a homologous spherical flow, we have $v = r/t$. For $t > 0$, the flow is an explosion ($v > 0$) starting with infinite density at $t = 0$. For $t < 0$, the flow is an implosion ($v < 0$) leading to infinite density at $t = 0$.

When Eq. (2.12) of Mihalas (1980) is applied to the homologous flow of matter with a grey extinction coefficient, the resulting frequency-integrated transfer equation is

$$\frac{\gamma}{c}(1 + \beta\mu)\frac{dI}{dt} + \frac{\mu}{\gamma ct}\frac{\partial I}{\partial\beta} + \frac{\gamma}{\beta ct}(1 - \mu^2)\frac{\partial I}{\partial\mu} + \frac{4\gamma}{ct}I = \eta - \chi I. \quad (1)$$

Here the dependent variable is the integrated specific intensity $I(\mu; \beta, t)$, the radial coordinate r has been replaced by $\beta = v/c$, the time derivative is Lagrangian, and $\gamma = 1/\sqrt{1-\beta^2}$.

2.2. Moment equations

Moment equations can be derived from Eq. (1) as usual by multiplying by $\frac{1}{2}\mu^m$ with $m = 0, 1, 2, \dots$ and then integrating over direction cosine μ . Alternatively, Eqs. (2.16) and (2.17) in Mihalas (1980) can be simplified to the case of homologous flow, as above for his transfer equation.

The resulting equations are

$$\frac{\gamma}{c} \frac{dJ}{dt} + \frac{\gamma\beta}{c} \frac{dH}{dt} + \frac{1}{\gamma ct} \frac{\partial H}{\partial \beta} + \frac{2\gamma}{\beta ct} (H + 2\beta J) = \eta - \chi J \quad (2)$$

for the zeroth moment, and

$$\frac{\gamma}{c} \frac{dH}{dt} + \frac{\gamma\beta}{c} \frac{dK}{dt} + \frac{1}{\gamma ct} \frac{\partial K}{\partial \beta} + \frac{\gamma}{\beta ct} (3K - J) = -\chi H \quad (3)$$

for the first moment.

Following Mihalas (1980), Eddington's flux variable H is here preferred to the standard flux $F = 4H$. The integrated physical flux in the cmf is therefore $\mathcal{F} = 4\pi H$.

Comparing Eqs. (2) and (3) with Eqs. (2.16) and (2.17) of Mihalas (1980), we see that specializing to homologous flow has resulted in a huge simplification in the coefficients of the moments J , H and K . Most notably, the coefficient of K in the zeroth moment equation reduces to zero, so now only J and H appear in this equation.

2.3. Separation of variables

In order to construct simple solutions of these equations for use in testing computer codes, we first effect a separation of variables. This is achieved by writing the specific intensity

$$I(\mu; \beta, t) = I_1(\mu; \beta) (t_1/t)^p \quad (4)$$

where t_1 is an arbitrary reference time, and the exponent p is unspecified. With this assumption, each term on the left-hand side of Eq. (1) scales as $(t_1/t)^{p+1}$. Accordingly, we must assume that

$$\eta(\beta, t) = \eta_1(\beta) (t_1/t)^{p+1} \quad (5)$$

and

$$\chi(\beta, t) = \chi_1(\beta) (t_1/t). \quad (6)$$

Not surprisingly, this necessary scaling of the extinction coefficient per unit volume implies that the ratio of $1/\chi$, the local mean free path of a photon, to the radius of the configuration is time-independent.

When Eqs. (4)–(6) are substituted in Eq. (1), the scaling factor cancels by construction, and we thus obtain the transfer equation

$$\frac{\mu}{\gamma ct_1} \frac{\partial I_1}{\partial \beta} + \frac{\gamma}{\beta ct_1} (1 - \mu^2) \frac{\partial I_1}{\partial \mu} + \frac{\gamma}{ct_1} [4 - p(1 + \beta\mu)] I_1 = \eta_1 - \chi_1 I_1 \quad (7)$$

that determines the scale-free radiation field $I_1(\mu; \beta)$.

The moments J , H and K evidently also scale as $(t_1/t)^p$. The equations satisfied by the corresponding scale-free moments $J_1(\beta)$, $H_1(\beta)$ and $K_1(\beta)$ are

$$\frac{1}{\gamma ct_1} \frac{dH_1}{d\beta} + \frac{\gamma}{\beta ct_1} (2 - p\beta^2) H_1 + \frac{\gamma}{ct_1} (4 - p) J_1 = \eta_1 - \chi_1 J_1 \quad (8)$$

for the zeroth moment, and

$$\frac{1}{\gamma ct_1} \frac{dK_1}{d\beta} - \frac{\gamma\beta}{ct_1} p K_1 + \frac{\gamma}{\beta ct_1} (3K_1 - J_1) + \frac{\gamma}{ct_1} (4 - p) H_1 = -\chi_1 H_1 \quad (9)$$

for the first moment.

Equations (7)–(9) are the basic equations of this investigation.

3. Testing a Monte Carlo code

If MC techniques are used directly to simulate the physics of radiation transport, then the MC quanta are photons and convergence to the solution of the Radiative Transfer Equation (RTE) requires that $\mathcal{N} \rightarrow \infty$, where \mathcal{N} is the number of photons whose interaction histories are followed. In such a code, in addition to crossings of boundaries, MC quanta are created spontaneously within the computational domain D by sampling the thermal emissivity and may subsequently be destroyed within D by absorption. Because the RTE is directly simulated, testing such MC codes is not fundamentally different from testing a conventional numerical solution of the RTE.

However, for transfer problems involving interactions between radiation and the internal energy states of matter, there are advantages in taking the MC quanta to be indestructible and indivisible energy (\mathcal{E} -) packets (Lucy 2003, and references therein). In such a code, in addition to crossings of boundaries, \mathcal{E} -packets are created spontaneously within D by sampling the *net* emissivity (i.e., emission minus absorption) but then, though the nature of the contained energy may change, they are not subsequently destroyed within D by absorption.

3.1. Moment solution

Let the integrated net emissivity per unit volume at time t_1 be $4\pi\tilde{\eta}_1$, where

$$\tilde{\eta}_1(\beta) = \eta_1 - \chi_1 J_1. \quad (10)$$

This quantity creates radiant energy within the configuration by a physical mechanism that need not be specified for test problems.

If we replace the right-hand side of Eq. (8) by $\tilde{\eta}_1$ and eliminate J_1 from the left-hand side by setting $p = 4$, the result is an ordinary differential equation (ODE) for $H_1(\beta)$,

$$\frac{dH_1}{d\beta} + \frac{2\gamma^2}{\beta} (1 - 2\beta^2) H_1 = \gamma c t_1 \tilde{\eta}_1. \quad (11)$$

This equation can be solved analytically with the integrating factor β^2/γ^2 . The solution satisfying the boundary condition $H_1(0) = 0$ is

$$H_1(\beta) = c t_1 \frac{\gamma^2}{\beta^2} \int_0^\beta \tilde{\eta}_1(b) b^2 \sqrt{1 - b^2} db. \quad (12)$$

Note that this formula is exact. In transfer theory, analytic formulae for moments are typically not exact because they are derived with Eddington's closure approximation $K = J/3$. Here this is not necessary: K and J drop out of the zeroth moment equation because of the assumptions of homologous flow and scaling exponent $p = 4$.

A second point to note is that $H_1(\beta)$ has been derived without specifying the scale-free extinction coefficient. Accordingly, Eq. (12) is valid for arbitrary $\chi_1(\beta)$.

It is of interest to note that the scaling $p = 4$ arises naturally in the limiting case of completely opaque matter within which there is no net emissivity. In this case, the right-hand side of Eq. (2) is zero, and the cmf flux $H = 0$ since radiation is position-coupled to matter. The solution of Eq. (2) is then such that $J \propto t^{-4}$, corresponding to adiabatic evolution of the radiation energy density present initially. In contrast, in the solution derived here, this same scaling is maintained because every layer's losses due to flux divergence is exactly replaced by the net emissivity in that layer. Moreover, the similarity solution represents the state reached when initial conditions have been erased.

3.2. A particular case

The simplest case for testing a MC code is when $\tilde{\eta}_1(\beta)$ is independent of β . This also simplifies the evaluation of the exact $H_1(\beta)$ since the integral in Eq. (12) is then analytic. The result is

$$H_1(\beta) = \frac{1}{8} c t_1 \tilde{\eta}_1 \frac{\gamma^2}{\beta^2} \left[\sin^{-1} \beta - \frac{\beta}{\gamma} (1 - 2\beta^2) \right]. \quad (13)$$

Thus we obtain an exact closed-form expression for the cmf flux in a particular time-dependent relativistic flow.

The corresponding moment $J_1(\beta)$ cannot be obtained exactly. But an approximate formula can be derived from Eqs. (9) and (13) with the help of Eddington's closure approximation and surface boundary condition. The resulting formula for J_1 can then be substituted in Eq. (10) to obtain an approximate formula for the conventional emissivity η_1 . Details are omitted.

3.3. Monte Carlo calculation

In order to illustrate how similarity solutions can be used to test codes, we now briefly report MC calculations for relativistic homologous flows. The MC code is a spherically-symmetric and fully relativistic version of the 3-D code described recently

(Lucy 2005). As in that code, the MC quanta are indestructible \mathcal{E} -packets. The calculations start at reference time t_1 with no \mathcal{E} -packets present. But as time advances, \mathcal{E} -packets spontaneously appear in accordance with the net emissivity $\tilde{\eta}_1(t_1/t)^5$ and then propagate through the configuration interacting with matter in accordance with extinction coefficient $\chi_1(t_1/t)$.

We choose to create equal numbers of \mathcal{E} -packets in equal intervals of $\log t$ and having cmf energies $\epsilon(t)$ that are independent of β . The energy dE created in the cmf within the space-time element $dV dt$ is $dE = 4\pi\tilde{\eta}dV dt$. But since $dV dt$ is invariant under the Lorentz transformation, we may regard $dV dt$ as referring to the rf. Accordingly, for the particular case (Sect. 3.2) where $\tilde{\eta}$ does not depend on β , the total cmf energy created in the rf interval dt is $4\pi\tilde{\eta}V dt$, where $V(t) = V(t_1)(t/t_1)^3$ is the rf volume at time t . Thus, if $dN/d\ell nt$ gives the packet creation rate, and we set $p = 4$, then the packets' cmf energies are

$$\epsilon(t) = 4\pi\eta_1 t_1 V_1 \left(\frac{t_1}{t} \right) \left(\frac{dN}{d\ell nt} \right)^{-1}. \quad (14)$$

With $\tilde{\eta}$ independent of β , $dE \propto dV$ at fixed rf t . Accordingly, since we choose ϵ to be independent of β , equal numbers of packets are created in equal rf volume elements. The appropriate MC sampling algorithm for the initial rf radius of a packet created at t is $r = R_* \sqrt[3]{z}$, where $R_* = c\beta_* t$ and z is a random number from $(0, 1)$. Here β_* is the value of v/c at the surface.

The transport of these packets through the configuration is as described in the earlier paper (Lucy 2005) except that now the factor γ in the Doppler formula is restored to make the code fully relativistic. The cmf energies of the packets that escape from the surface in each rf time step Δt are summed and then divided by $\Delta t/\gamma_*$ to obtain an estimate of the cmf luminosity $L(t)$.

Monte Carlo simulations for two strongly relativistic explosions are plotted in Fig. 1. For these simulations, the rf time steps are $\Delta \log t = 0.02$, during each of which $N = 1000$ additional \mathcal{E} -packets are created with cmf energies given by Eq. (14).

The evolution of the cmf luminosity is shown starting at t_1 , together with the predicted result $L = 4\pi R_*^2 \times 4\pi H_1(\beta_*) \times (t_1/t)^4$, with $H_1(\beta_*)$ from Eq. (13). One solution is the free streaming limit ($\chi_1 = 0$) and the second ($\chi_1 = 3$) has photon mean free paths $= R_*(t)/3$. In both cases, the MC solutions tend asymptotically to the similarity solution, the convergence being somewhat slower for $\chi_1 = 3$ because of the longer residence times of the \mathcal{E} -packets. Since agreement is achieved in both cases, the prediction, for $p = 4$, that the cmf flux H is independent of χ_1 is confirmed.

3.4. Relativistic implosions

Although relatively trivial, it is of interest to illustrate the application to implosions. Accordingly, Fig. 2 shows the same two test problems but with the signs of t_1 and β_* reversed. Again, after a transition period during which the internal radiation field is established, the MC solutions converge to the similarity solution.

This possibility of testing numerical treatments of radiative transfer in relativistic implosions is possibly relevant for codes

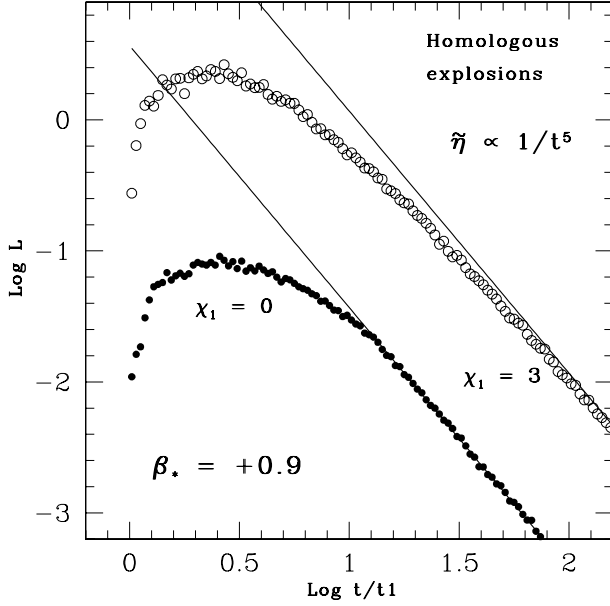


Fig. 1. Explosions. Comparison of MC calculations (*circles*) of the cmf luminosity $L(t)$ with predictions of similarity theory (*straight lines*). The surface velocity $v_s = 0.9c$. The unit for the indicated scale-free extinction coefficients χ_1 is $1/R_1$, where $R_1 = v_s t_1$. The unit of luminosity is $4/3\pi R_1^3 \times 4\pi\tilde{\eta}_1$. The luminosities for $\chi_1 = 3$ have been increased by 1.5 dex.

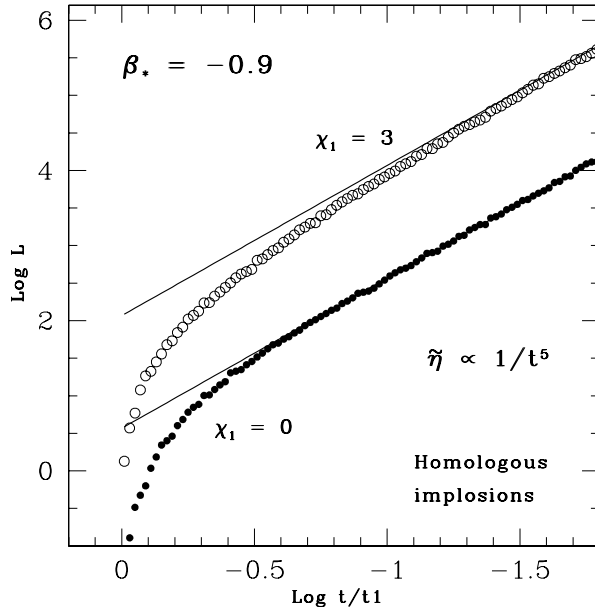


Fig. 2. Implosions. Same as Fig. 1 but with signs reversed for β_* and t_1 . The luminosities for $\chi_1 = 3$ have been increased by 1.5 dex.

that simulate laser-driven implosions in support of the quest for fusion by inertial confinement.

Accurate numerical solutions for relativistic inflows have also been computed by Yin & Miller (1995), who stress the dramatic effects that can arise from photon trapping. But their solutions are only for stationary flows.

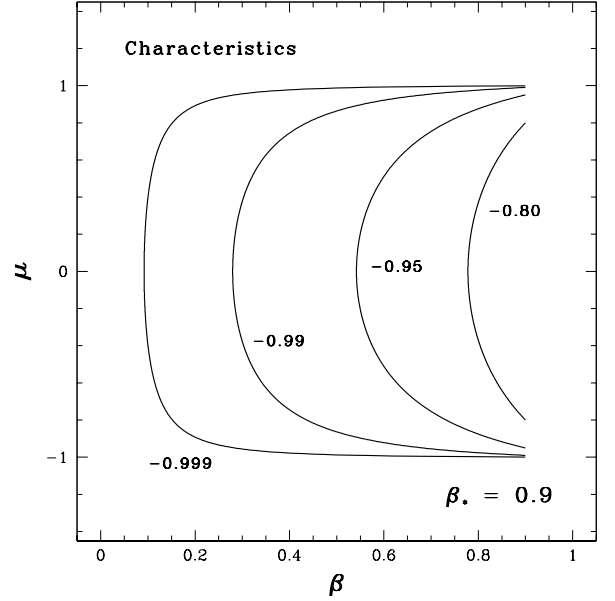


Fig. 3. Characteristic trajectories $\mu(\beta; \mu_*)$ for Eq. (7) when $\beta_* = 0.9$. The curves are labelled with the value of μ_* , the direction cosine at the surface for the inward ray.

4. Testing a transfer code

Apart from the degenerate case $\chi_1 = 0$, the exact solution of Sect. 3 is not appropriate for the precision testing of a conventional relativistic transfer code since the implied scale-free emissivity η_1 could only be determined approximately. Accordingly, we now seek exact solutions when η_1 is specified rather than $\tilde{\eta}_1$.

4.1. Solution along characteristics

As did Mihalas (1980, Sect. IIIb) for his general equation, we construct characteristics for Eq. (7) such that the partial differential operator becomes a perfect differential. Thus Eq. (7) becomes

$$\frac{1}{ct_1} \frac{dI_1}{ds} + \left[\chi_1 - \frac{(p-4)\gamma + p\gamma\beta\mu}{ct_1} \right] I_1 = \eta_1 \quad (15)$$

where $ct_1 s$ is distance along a characteristic defined by the equations

$$\frac{d\beta}{ds} = \frac{\mu}{\gamma} \quad \text{and} \quad \frac{d\mu}{ds} = \frac{\gamma}{\beta} (1 - \mu^2). \quad (16)$$

Dividing these equations, we find that $\gamma\beta\sqrt{1-\mu^2}$ is constant along characteristics. Accordingly, the family of characteristics is given by

$$\gamma\beta\sqrt{1-\mu^2} = \gamma_*\beta_*\sqrt{1-\mu_*^2} = \alpha \quad (17)$$

where $-1 < \mu_* < 0$ is a characteristic's direction cosine at its entry point into the configuration. Integrations of Eq. (15) proceed inwardly along such characteristics starting at $s = 0$ with the boundary condition $I_1(\mu_*; \beta_*) = 0$ and continuing until the characteristic emerges at the surface with $\mu = |\mu_*|$.

In Fig. 3, the characteristics are plotted for various values of μ_* when $\beta_* = 0.9$. Note that, to obtain a characteristic that

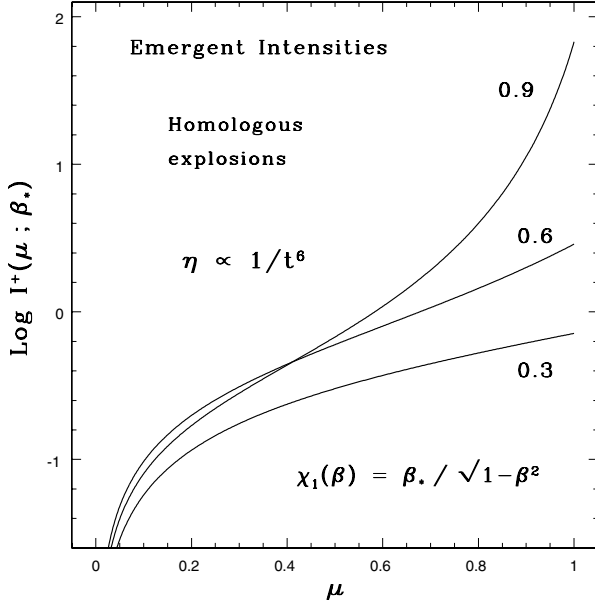


Fig. 4. Emergent intensities in the co-moving frame for the indicated values of β_* . The exponent $p = 5$, and χ_1 is from Eq. (24). The formula for $\chi_1(\beta)$ in units of $1/R_1$ is exhibited (cf. Figs. 1 and 2). The unit of intensity is $ct_1\eta_1$.

penetrates close to the centre, the parameter μ_* must closely approach -1 . The point of closest approach ($\mu = 0$) is at $\gamma = \sqrt{1 + \alpha^2} = \gamma_0$, or, equivalently, at $\beta = \alpha/\gamma_0 = \beta_0$.

Parenthetically, we note that these analytic characteristic curves provide a further powerful test of the relativistic MC code described in Sect. 3.3. In the free streaming case, each \mathcal{E} -packet follows its appropriate characteristic to high precision, as it should. At creation, an \mathcal{E} -packet's initial β and μ determine its invariant $\gamma\beta\sqrt{1-\mu^2}$ and hence μ_* from Eq. (17). The packet then propagates along this characteristic in the direction of increasing s until it escapes at the surface $\beta = \beta_*$ with $\mu = |\mu_*|$.

The simplicity of the characteristics for homologous flow allows the dimensionless arc length s to be evaluated analytically as a function of β . Integrating the first member of Eq. (16) after eliminating μ with Eq. (17), we find that, along the inwardly-directed ($\mu < 0$) segment of a characteristic,

$$s(\beta; \mu_*) = \frac{1}{\gamma_0} \left[\sin^{-1} \left(\frac{\gamma_0}{\gamma} \right) - \sin^{-1} \left(\frac{\gamma_0}{\gamma_*} \right) \right]. \quad (18)$$

The corresponding formula after the point of closest approach ($\mu > 0$) is

$$s(\beta; \mu_*) = \frac{1}{\gamma_0} \left[\pi - \sin^{-1} \left(\frac{\gamma_0}{\gamma} \right) - \sin^{-1} \left(\frac{\gamma_0}{\gamma_*} \right) \right]. \quad (19)$$

Because the function $s(\beta; \mu_*)$ is readily inverted to give $\beta(s; \mu_*)$, the remaining quantities γ , μ , $\eta_1(\beta)$ and $\chi_1(\beta)$ can likewise be transformed into functions of s along the characteristic defined by μ_* for the given β_* ; and this remark therefore applies also to the coefficient of I_1 in Eq. (15).

Let us now define the effective extinction coefficient along a characteristic to be

$$\hat{\chi}_1(s; \mu_*) = \chi_1 - \frac{(p-4)\gamma + p\gamma\beta\mu}{ct_1} \quad (20)$$

with corresponding effective optical depth

$$\hat{\tau}_1(s; \mu_*) = ct_1 \int_0^s \hat{\chi}_1 ds. \quad (21)$$

In terms of these quantities, the formal solution of Eq. (15) subject to the boundary condition $I = 0$ at $s = 0$ is

$$I_1(s; \mu_*) = ct_1 \int_0^s \eta_1(s') e^{\hat{\tau}(s') - \hat{\tau}(s)} ds'. \quad (22)$$

With straightforward numerical integrations, Eqs. (18)–(22) allow the intensity $I(s; \mu_*)$ to be determined as a function s along the characteristic defined by μ_* . By varying μ_* from -1 to 0 , we can thus determine I throughout the (μ, β) -plane.

This reduction of the problem to solution with the formal integral strongly suggests that these results could also be obtained with the method developed by Baschek et al. (1997). Although their paper is restricted to stationary relativistic flows, they note that time-dependent problems can be treated.

4.2. Equivalent static medium

The above analysis shows that, with the scaling assumptions for η and χ given in Eqs. (5) and (6), the time-dependent relativistic transfer problem for homologous spherical flow, reduces asymptotically to a transfer problem in a static medium. For explosions, the solution tends to this asymptote as $t \rightarrow \infty$; for implosions, the limit is $t \rightarrow 0$. For free-streaming, the similarity solution is achieved after all light signals emitted from within the configuration at $t = t_1$ have escaped.

Because light travel-time and relativistic effects are absent in a static medium, these effects reappear in Eq. (20) as corrections to the extinction coefficient. The term $\propto(p-4)$, which survives in the limit $\beta \rightarrow 0$, represents the combination of finite propagation speed and the time-dependence of the emissivity. The second correction term, which $\rightarrow 0$ as $\beta \rightarrow 0$, represents relativistic effects.

Note that these corrections can give $\hat{\chi}_1 < 0$, which implies that $\hat{\tau}_1$ is not necessarily a monotonically increasing function of s . Accordingly, $\hat{\tau}_1$ is not appropriate as an alternative independent variable for Eq. (15).

4.3. A particular case: Moment solution

Although the analysis of Sect. 4.1 provides a complete solution for the scale-free radiation field without assumptions about $\eta_1(\beta)$ or $\chi_1(\beta)$, the answer is not in closed analytic form as was the earlier result (Eq. (13)) for the cmf flux H_1 when the net emissivity $\tilde{\eta}$ is independent of β . Interestingly, an analogous result can be constructed when the conventional emissivity η is the quantity specified.

The coefficient of J_1 in Eq. (8) is zero if we set

$$\chi_1(\beta) = (p-4) \frac{\gamma}{ct_1}. \quad (23)$$

Thus $p > 4$ is necessary for $\chi_1 > 0$, while $p = 4$ gives free-streaming radiation.

With χ_1 given by Eq. (23), Eq. (8) simplifies to

$$\frac{dH_1}{d\beta} + \frac{\gamma^2}{\beta}(2 - p\beta^2)H_1 = ct_1\gamma\eta_1. \quad (24)$$

This equation has integrating factor β^2/γ^{p-2} , and so the solution satisfying the boundary condition $H_1(0) = 0$ is

$$H_1(\beta) = ct_1 \frac{\gamma^{p-2}}{\beta^2} \int_0^\beta \eta_1(b) b^2 (1 - b^2)^{\frac{p-3}{2}} db. \quad (25)$$

A simple case for which this integral is analytic is obtained by assuming that η_1 is independent of β and that $p = 5$. The result is

$$H_1(\beta) = \frac{1}{15} ct_1 \eta_1 \gamma^3 \beta (5 - 3\beta^2). \quad (26)$$

With this exact formula, a code that solves relativistic transfer problems with conventional techniques can be subjected to tests similar to those described in Sect. 3.3 for a MC code based on \mathcal{E} -packets.

4.4. A particular case: Complete solution

The particular case of Sect. 4.2 is remarkable in that the complete solution can be obtained in closed form. The starting point is Eq. (15) with χ_1 from Eq. (23). The independent variable s is conveniently transformed to β using the first member of Eq. (16). The resulting transfer equation is

$$\frac{dI_1}{d\beta} - p\gamma^2\beta I_1 = ct_1\eta_1 \frac{\gamma}{\mu} \quad (27)$$

where, from Eq. (17),

$$\mu(\beta) = \pm \frac{\gamma_0}{\beta} \sqrt{\beta^2 - \beta_0^2}. \quad (28)$$

Here the negative root applies along the inward segment of a characteristic as β decreases from β_* to β_0 – see Fig. 3. Thereafter, the positive root applies.

The integrating factor for Eq. (27) is γ^{-p} . Accordingly, substituting for μ , imposing boundary condition $I^-(\beta_*) = 0$, setting $p = 5$, and assuming that η_1 is independent of β , we find that the intensity of inwardly-directed radiation is

$$I^-(\beta; \mu_*) = ct_1\eta_1 \frac{\gamma^5}{\gamma_0} \int_\beta^{\beta_*} \frac{(1 - b^2)^2}{\sqrt{b^2 - \beta_0^2}} b db \quad (29)$$

which simplifies to

$$I^-(\beta; \mu_*) = ct_1\eta_1 \frac{\gamma^5}{\gamma_0} [g(\beta_*; \mu_*) - g(\beta; \mu_*)] \quad (30)$$

where

$$g(\beta; \mu_*) = \xi \left(\frac{1}{\gamma^4} + \frac{4}{3} \frac{\xi^2}{\gamma^2} + \frac{8}{15} \xi^4 \right) \quad (31)$$

with

$$\xi(\beta; \mu_*) = \sqrt{\beta^2 - \beta_0^2}. \quad (32)$$

The outwardly-directed intensity is obtained similarly. In this case, the boundary condition is $I^+(\beta_0; \mu_*) = I^-(\beta_0; \mu_*)$, and the solution is

$$I^+(\beta; \mu_*) = ct_1\eta_1 \frac{\gamma^5}{\gamma_0} [g(\beta_*; \mu_*) + g(\beta; \mu_*)]. \quad (33)$$

Equations (30) and (33) determine the intensity along the characteristic defined by μ_* . But these formulae can readily be used to calculate $I_1(\mu; \beta)$, the intensity as a function of μ at fixed β . Given μ and β , Eq. (17) determines α , which in turn determines β_0 , so that $\beta_0 = \beta_0(\mu, \beta)$ and similarly of course for γ_0 . Thus the right-hand sides of Eqs. (30) and (33) are now functions of μ and β , and the characteristics are no longer relevant.

This exact closed form analytic solution has been checked by substitution back into Eq. (7) using numerical differentiation to evaluate the two partial derivatives.

In Fig. 4, the emergent intensity given by Eq. (33) is plotted for various values of β_* . This shows extremely strong forward peaking when $\beta_* = 0.9$, with huge intensities when $\mu \gtrsim 0.9$. This is basically a light travel-time effect: with $\beta_* = 0.9$, radiation emerging with $\mu \sim 1$ includes photons emitted shortly after the explosion when, since $j \propto 1/t^6$, the emissivity was much higher than that now in the surface layers.

One consequence of this forward peaking is poor accuracy for Eddington's approximations. Thus, at the surface of the $\beta_* = 0.9$ solution, $K_1/J_1 = 0.821$ and $H_1/J_1 = 0.895$, as against Eddington's values of $1/3$ and $1/2$, respectively.

4.5. A particular case: Thermal emission

Thus far the physical mechanisms responsible for extinction and emission have not been specified. But let us now suppose that

$$\chi = k + \sigma \quad (34)$$

where k and σ are grey absorption and scattering coefficients, respectively. The corresponding integrated emissivity coefficient is then

$$\eta = kB + \sigma J \quad (35)$$

where B is the integrated Planck function, and the scattering is isotropic in the cmf.

Equations (34) and (35) are consistent with the scaling of Eqs. (5) and (6) if k and σ are $\propto 1/t$ and if $B \propto 1/t^p$. Given these scalings, the exact solution of Sect. 4.4 can now be applied as follows: we set $p = 5$ and choose the scale-free functions $k_1(\beta)$ and $\sigma_1(\beta)$ such that their sum satisfies Eq. (23). Then, since $J_1(\beta)$ can be computed from Eqs. (30) and (33), the implied scale-free function $B_1(\beta)$ can be derived from Eq. (35). Because the thermal emissivity is now known, this analytic solution can be used to test a code that incorporates an iteration procedure to determine the scattering contribution to the emissivity.

The net emissivity $\tilde{\eta}_1 = \eta_1 - \chi_1 J_1 = k(B_1 - J_1)$ is also determined by the above steps. Accordingly, this analytic solution can be used to test MC codes based on \mathcal{E} -packets. Moreover, this test is in principle more powerful than that provided by the flux moment solution of Sect. 3.2 since the angular distribution of the MC radiation field can now also be checked.

5. Conclusion

The aim of this paper has been to derive exact analytic solutions in order to test radiative transfer codes for relativistic flows. Such solutions exist for spherically-symmetric homologous flows with power-law time dependencies for the grey extinction coefficient and the integrated emissivity. The exact solution for the integrated intensity derived in Sect. 4.4, being a function of three independent variables t, μ, β and one parameter β_* , provides an extraordinarily demanding and informative test for such codes. Moreover, its somewhat contrived derivation based on a particular spatial variation of χ in no way lessens its usefulness.

In addition to deriving closed form analytic formulae for the intensity and flux in the cmf, an exact formula has been derived for the characteristics. This allows the kinematic and geometric aspects of relativistic transport codes to be tested independently of the treatments of absorption and emission. For MC codes, this test is carried out by setting the extinction coefficient to zero and then checking that photon packets propagate along the known characteristics.

In solving time-dependent transport problems with the RTE, the time derivatives are commonly approximated with a backward difference formula, thus using the solution at the previous time step. This introduces errors $O(\Delta t)$ that might well accumulate as the integration proceeds. With the availability of an exact time-dependent solution, the magnitude of the accumulated error can be determined. If the error accumulation is unacceptable, a higher order difference formula can be employed that uses the solutions at the two previous time steps (Lucy 2005).

References

- Baschek, B., Efimov, G. V., von Waldenfels, W., & Wehrse, R. 1997, *A&A*, 317, 630
- Castor, J. I. 1972, *ApJ*, 178, 779
- Lucy, L. B. 2003, *A&A*, 403, 261
- Lucy, L. B. 2005, *A&A*, 429, 19
- Mihalas, D. 1980, *ApJ*, 237, 574
- Prokof'ev, V. A. 1962, *Soviet Phys. – Doklady*, 6, 861
- Yin, W.-W., & Miller, G. S. 1995, *ApJ*, 449, 826